

Directed Biosynthesis of Mitragynine Stereoisomers

Carsten Schotte,¹ Yindi Jiang,¹ Dagny Grzech, Thu-Thuy T. Dang, Larissa C. Laforest, Francisco León, Marco Mottinelli, Satya Swathi Nadakuduti, Christopher R. McCurdy, and Sarah E. O'Connor*



Cite This: *J. Am. Chem. Soc.* 2023, 145, 4957–4963



Read Online

ACCESS |

Metrics & More

Article Recommendations

Supporting Information

ABSTRACT: *Mitragyna speciosa* (“kratom”) is used as a natural remedy for pain and management of opioid dependence. The pharmacological properties of kratom have been linked to a complex mixture of monoterpene indole alkaloids, most notably mitragynine. Here, we report the central biosynthetic steps responsible for the scaffold formation of mitragynine and related corynanthe-type alkaloids. We illuminate the mechanistic basis by which the key stereogenic center of this scaffold is formed. These discoveries were leveraged for the enzymatic production of mitragynine, the C-20 epimer speciogynine, and fluorinated analogues.

Mitragyna speciosa (“kratom”) is a tree of the *Rubiaceae* family. Kratom consumption leads to stimulating effects at lower doses and opioid-like effects at higher doses.¹ Manual workers have used it for centuries to endure heat and combat fatigue.^{2,3} Kratom is also consumed for the (self)treatment of pain, to mitigate opioid withdrawal symptoms, and to treat depression; however, rigorous clinical demonstration of kratom’s therapeutic efficacy is still lacking.⁴ Because of its purported analgesic properties, as well as for recreational purposes, kratom is increasingly used worldwide and is consumed by millions of people in the United States alone.^{5,6}

The pharmacological effects of kratom have been linked to a mixture of >50 corynanthe- and oxindole-type alkaloids (Figure 1a,b).⁷ Most notable among these are the corynanthe-type alkaloid mitragynine (1) and the hydroxylated derivative 7OH-mitragynine (2). Both 1 and 2 are nanomolar partial agonists at the human μ -opioid receptor (hMOR), and 2 was found to be ~10-fold more potent than morphine in mice.^{8,9} Intriguingly, speciogynine (3), the C-20 epimer of mitragynine (1), does not display agonist activity toward hMOR, though speciogynine (3), unlike mitragynine (1), is a smooth muscle relaxant. These differential bioactivities highlight the importance of the C-20 stereochemistry in the pharmacology of kratom alkaloids.¹⁰

Here, we leverage a multiomics approach to elucidate the key biosynthetic steps that form the corynanthe-type scaffold of kratom alkaloids. We report the discovery of two medium-chain alcohol dehydrogenases (*MsDCS1* and *MsDCS2*) along with an enol *O*-methyltransferase (*MsEnolMT*) that converts strictosidine aglycone (4) to either (20S)-corynantheidine (5a) (the precursor to 1) or (20R)-corynantheidine (5b) (the precursor to 3). Rational mutagenesis of *MsDCS1* revealed key amino acid residues that control the stereoselective reduction at C-20. A precursor directed biosynthesis approach was then used for the stereoselective production of 1 and 3, as well as fluorinated analogues.

We first identified where these alkaloids accumulate in *planta* by analyzing methanolic extracts of *M. speciosa* root, stem, bark, and leaf tissue using targeted metabolomics (Figure 1c; Figures

S1–S6). Consistent with literature reports^{11,12} the alkaloid content in the leaves was higher than other organs, with mitragynine (1), paynantheine (6), speciogynine (3), and speciocilliatine (7) being the dominant products. Low levels of 7OH-mitragynine (2), (20S)-corynantheidine (5a), and strictosidine (8) were also observed. Stem and bark showed similar metabolic profiles, with 7 as the dominant alkaloid and low quantities of 1 and 3 also observed. Notably, root tissue was completely lacking in 1 and 3, with only 7, 8, and 5a detected.

Strictosidine aglycone (4) is the central intermediate for most monoterpene indole alkaloids, including 1, 3, and other kratom-derived alkaloids. The biosynthetic pathway for 4 has been elucidated in *Catharanthus roseus*,¹³ and we identified orthologues of these biosynthetic genes in the kratom transcriptome (Scheme 2a). Notably, although 1 and 3 accumulate primarily in leaf and stem, the strictosidine aglycone (4) biosynthetic genes were preferentially expressed in roots, suggesting that this organ is the primary site of biosynthesis for the early pathway steps toward 1. Therefore, either 1 and 3 are produced in the root and subsequently transported to leaf/stem, or alternatively, a biosynthetic intermediate of 1 and 3 is transported to the leaf/stem where the final biosynthetic steps would take place.

Strictosidine aglycone (4) is a reactive intermediate that can be reductively trapped into numerous isomers.^{14,15} One isomer, dihydrocorynantheine (11ab), has the same scaffold as 1 and 3, and is therefore a likely biosynthetic intermediate for these alkaloids. Recently, we reported the discovery of a medium-chain alcohol dehydrogenase from *Cinchona pubescens*, dihydrocorynantheine synthase (*CpDCS*), that converts strictosidine aglycone (4) to (20R)-dihydrocorynantheine

Received: December 22, 2022

Published: February 22, 2023



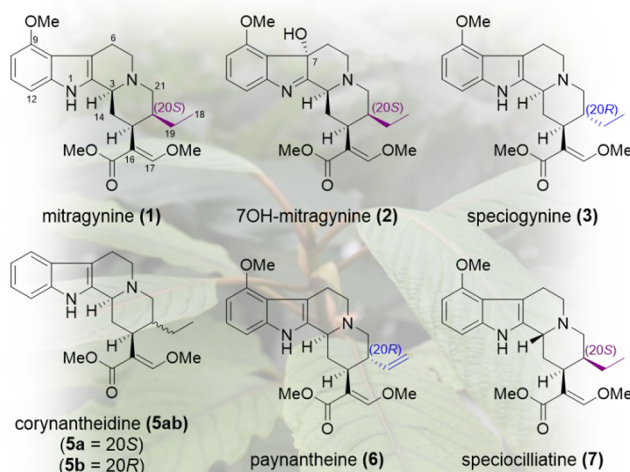
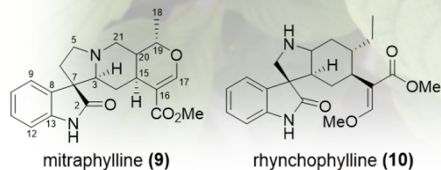
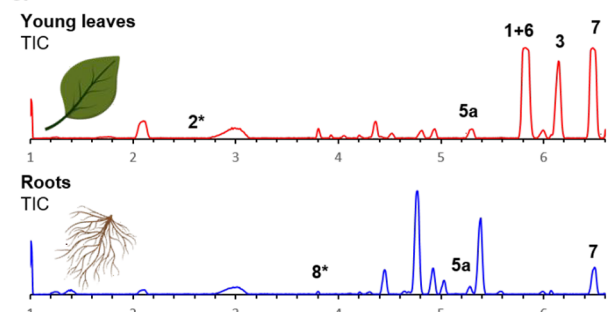
a. corynanthe-type alkaloids**b. oxindole-type alkaloids****c.**

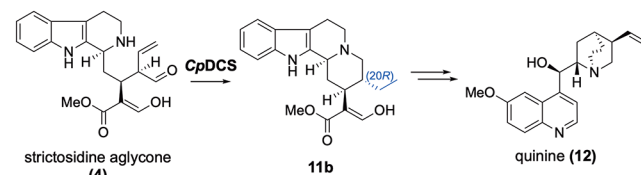
Figure 1. (a, b) Representative kratom alkaloids. (c) TIC of kratom leaf and root extracts. * observed in EIC.

(11b) during the biosynthesis of quinine (12) (**Scheme 1a**). The structure of 11b was inferred based on (HR)MS/MS experiments and by NMR characterization of the decarboxylated product (20R)-dihydrocorynantheal (Figure S7).¹⁶ It seemed logical that orthologous enzymes should catalyze the reduction of strictosidine aglycone to the dihydrocorynantheine scaffold in kratom (**Scheme 1b**).^{16,17} Moreover, given the presence of dihydrocorynantheine-like alkaloids with both (20S)- and (20R)-stereochemistry in kratom, we further hypothesized that kratom would have multiple DCS orthologues with differing stereoselectivity.

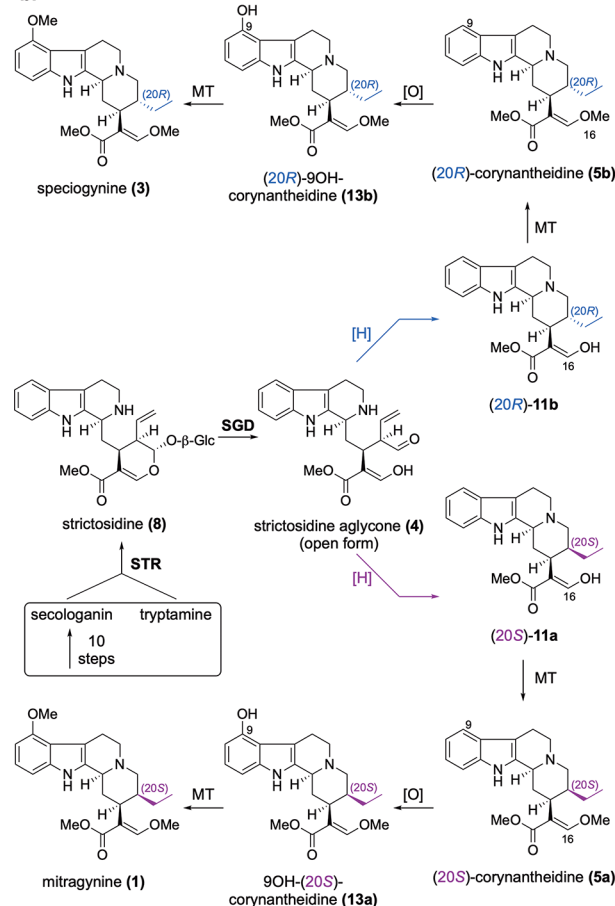
To identify enzyme candidates from kratom that catalyze formation of 11a or 11b from strictosidine aglycone (4), we used the protein sequence of CpDCS to mine the kratom transcriptome. From this process, 27 candidates that showed homology to CpDCS and/or coexpressed with genes involved in (8)-formation were expressed in *Escherichia coli* (Figures S8 and S9). To assay for enzymatic activity, strictosidine (8) was deglycosylated *in situ* with strictosidine glucosidase from *C. roseus* (CrSGD) and incubated with kratom reductase candidates and NADPH. CpDCS, which afforded (20R)-dihydrocorynantheine (11b),¹⁶ was used as a positive control

Scheme 1. (a) Reduction of 4 by CpDCS and (b) Proposed Pathway Toward Major Kratom Alkaloids

a.



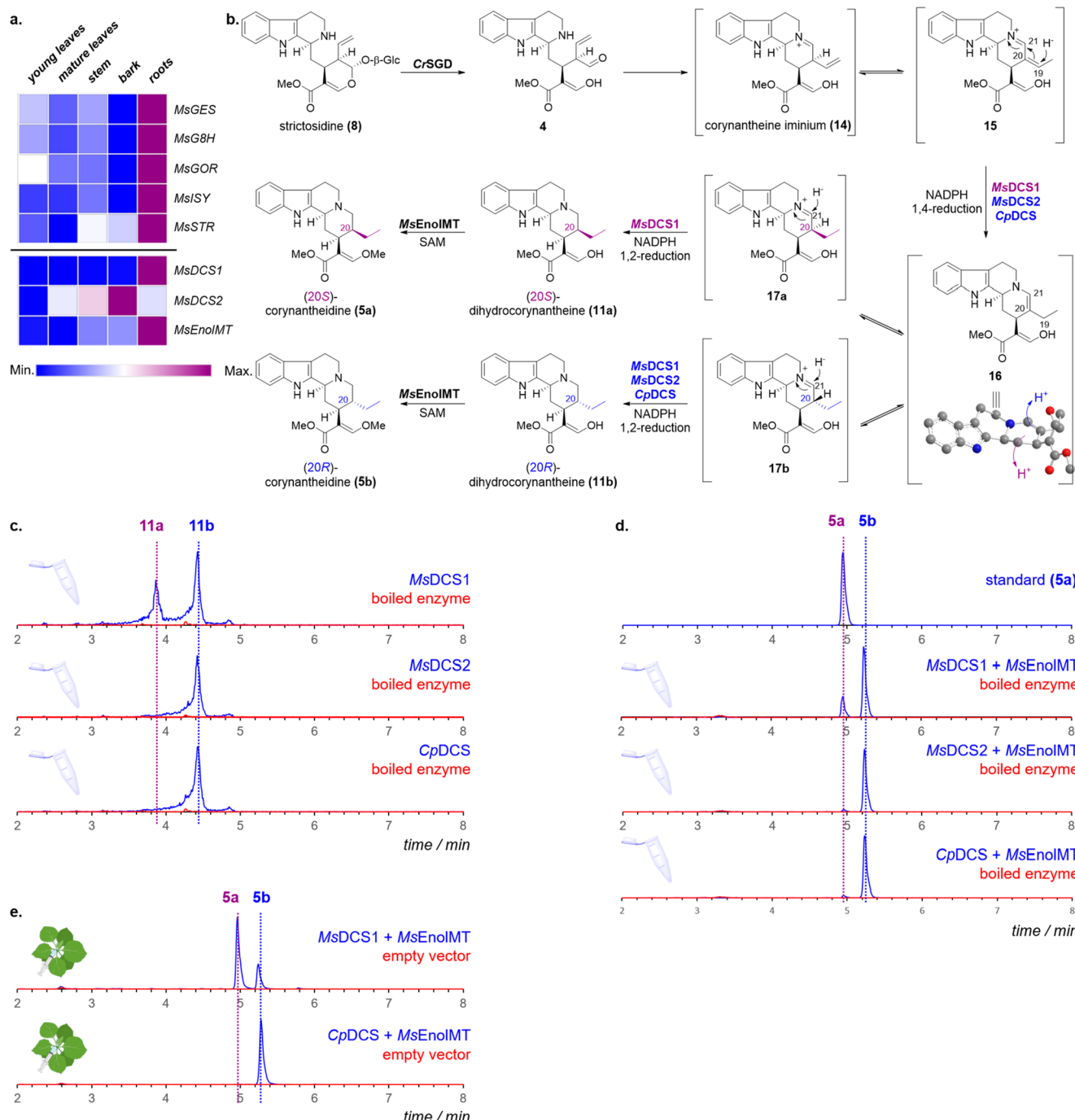
b.



(**Scheme 2c**; $T_R = 4.4$ min; $[M + H]^+$ calcd for $C_{21}H_{27}N_2O_3$, 355.2022; found, 355.2014).¹⁶ Two of the tested kratom candidates, MsDCS1 and MsDCS2, also produced 11b (**Scheme 2c**; **Figure S10**). Intriguingly, MsDCS1 also yielded a second product with the same HRMS ($[M + H]^+$ calcd for $C_{21}H_{27}N_2O_3$, 355.2022; found, 355.2015) and MS/MS fragmentation pattern as 11b, but a different retention time ($T_R = 3.9$ min; **Scheme 2c**; **Figure S10**). We assumed that this product was (20S)-dihydrocorynantheine (11a), but due to poor stability, this compound could not be characterized.

Subsequent O-methylation at C-16 of 11ab would yield corynantheidine (5ab), which is the next predicted intermediate in the biosynthesis of 1 and 3. To identify gene candidates that catalyze O-methylation at C-16 of 11ab, we identified annotated methyltransferase genes that coexpress with MsDCS1 ($r > 0.8$, Pearson correlation coefficient). Five purified enzyme candidates were assayed *in vitro* with strictosidine (8), strictosidine glucosidase (CrSGD), NADPH, SAM, and either CpDCS, MsDCS1, or MsDCS2. A single enzyme, MsEnolMT ($r = 0.96$), showed methyltransfer-

Scheme 2. (a) Expression Profiles of Identified Genes in Kratom;^a (b) Proposed Mechanism for the Formation of the Corynanthe-Type Skeleton; (c) EIC ($m/z = 355$) of Assays Featuring Combinations of 8, CrSGD, and MsDCS1/MsDCS2/CpDCS; (d) EIC ($m/z = 369$) of Assays Featuring Combinations of 8, CrSGD, MsEnolMT, and MsDCS1/MsDCS2/CpDCS; and (e) EIC ($m/z = 369$) Corresponding to Transient Expression of CrSTR, CrSGD, MsDCS1/CpDCS, and MsEnolMT in Tobacco



^aExpression levels are represented as FPKM of the *M. speciosa* transcriptome.

ase activity in all enzyme assays (Scheme 2d). Coincubation of MsEnolMT with MsDCS1 afforded two products with the expected nominal mass of 368 corresponding to the methylated product of 11ab (HRMS: $[M + H]^+$ calcd for $C_{22}H_{28}N_2O_3$, 369.2178; found, 369.2164 and 369.2167). The minor product ($T_R = 4.9$ min) eluted at the same retention time and displayed identical MS/MS spectra compared to an authentic standard of 5a (Figures S11 and S12),¹⁸ validating

that MsDCS1 generates (20S)-dihydrocorynantheine (11a). The major product 5b ($T_R = 5.4$ min) displayed identical MS/MS patterns to 5a (Figure S12), but different retention time. This product has the same retention time and MS/MS pattern as the product of CpDCS, which had been previously established to have R stereoselectivity (Scheme 2c,d).¹⁶ Moreover, the MS/MS and the retention time of the decarboxylated major MsDCS1 product matched an authentic

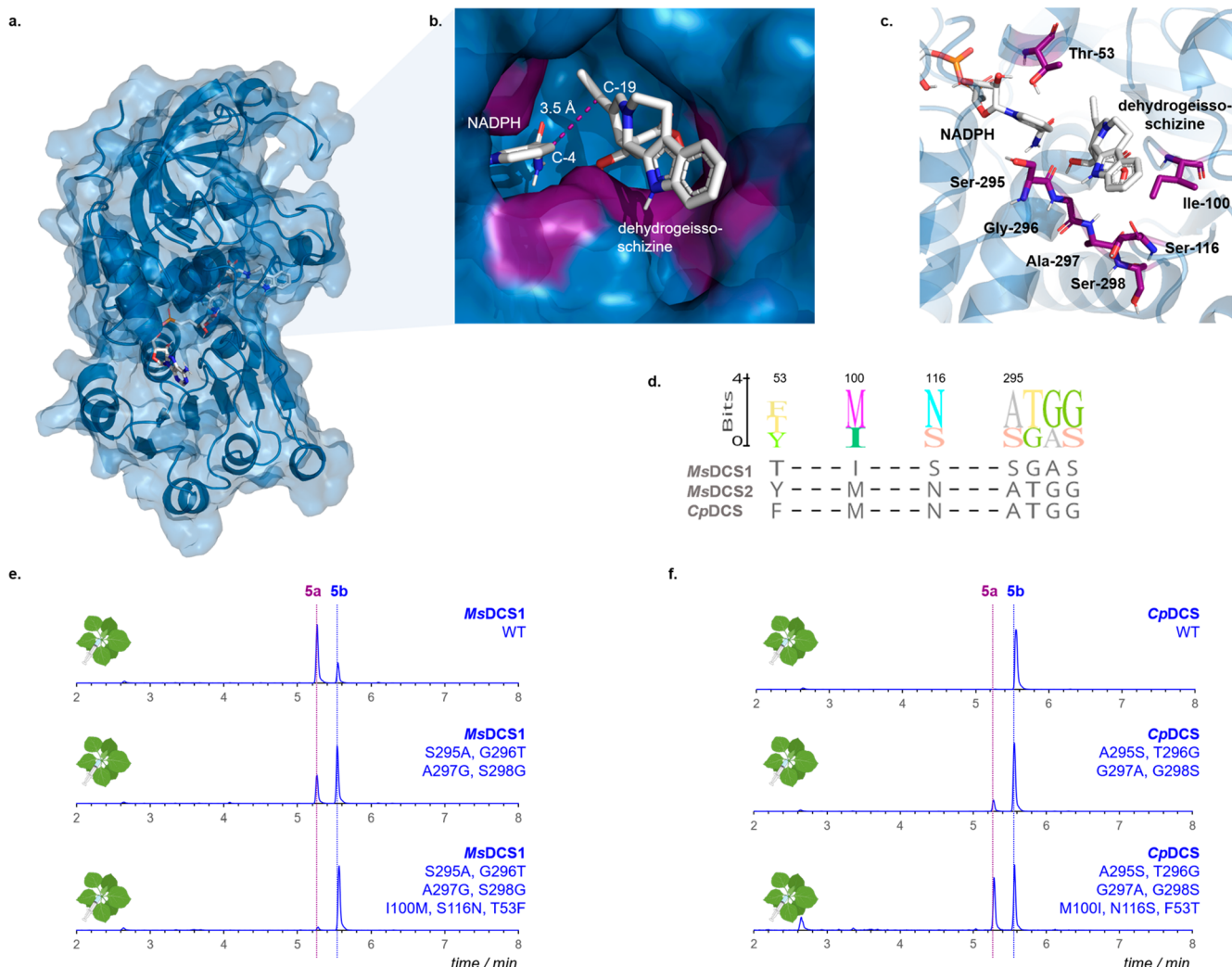


Figure 2. (a, b) Structural model of MsDCS1 in complex with NADPH and dehydrogeissoschizine (**15**). (c) Key active site residues directing the stereoselectivity. (d) Sequence alignment between MsDCS1, MsDCS2, and CpDCS. (e, f) Levels of (*20S*)-**5a** and (*20R*)-**5b** in mutants of MsDCS1/CpDCS; displayed are EICs (*m/z* 369) corresponding to transient expression of CrSTR, CrSGD, and ADH mutants and MsEnolMT in *Nicotiana benthamiana*.

standard of (*20R*)-dihydrocorynantheal (Figure S7).¹⁶ MsDCS1 also showed *R* stereoselectivity (Scheme 2c).

The ratios of **11a** and **11b** produced by MsDCS1 varied considerably among *in vitro* assays, suggesting that assay conditions affect the stereochemical outcome. To corroborate MsDCS1 activity, we transiently expressed MsDCS1 together with CrSTR, CrSGD, and MsEnolMT in *Nicotiana benthamiana* leaves. Infiltration with tryptamine and secologanin (**19**) [the precursors to strictosidine (**8**)] afforded reproducible ratios of **5a** and **5b**, with **5a** as the dominant product (Scheme 2e). Exchange of MsDCS1 with CpDCS afforded solely **5b**, in agreement with previous observations.

Formation of **11ab** may likely proceed via an initial 1,4-reduction of the α,β -unsaturated iminium dehydrogeissoschizine (**15**), which can form *in situ* upon deglycosidation of **8** (Scheme 2b).¹⁶ The reduced intermediate **16** tautomerizes to the iminium form, **17ab**, upon protonation at C-20, after which a second 1,2-reduction would occur at C-21. Protonation at C-20 during tautomerization would therefore define the stereochemical outcome. We hypothesized that differences within the active site of these enzymes controlled the face of protonation.

To identify candidate amino acid residues that direct the C-20 stereochemistry, we generated a structural model of MsDCS1 (Figure 2a–c).^{19,20} Seven amino acids in the binding pocket differentiate MsDCS1 from MsDCS2/CpDCS (Figure 2c,d; Figure S13). These residues from MsDCS2/CpDCS were introduced into MsDCS1 to swap stereoselectivity at C-20. Assays were performed by transient expression of the resulting mutants in tobacco leaves (together with CrSTR, CrSGD, MsEnolMT, tryptamine, and secologanin; Figure 2e; Figure S14). Mutagenesis of residues 295–298 (SGAS to ATGG) was sufficient to invert the ratio between **5a** and **5b** (from ~74% **5a** in wild-type MsDCS1 to <35% **5a** in the mutant). In a septuple mutant of MsDCS1 (T53F, I100M, S116N, SGAS295–298ATGG), formation of the (*20S*)-isomer **5a** was nearly abolished (<5%). Similar results were observed in analogous mutations in CpDCS, which forms the (*20R*) product **5b** (Figure 2f). In the septuple CpDCS mutant (F53T, M100I, N116S, ATGG295–298SGAS), the amount of **5a** changed to ~45% in the mutant compared to 0% in the wild type enzyme (Figure 2f; compare to Figure S14 for additional mutations). Mining of the kratom genome revealed that MsDCS1 is the only homologue harboring these residues at these positions, so

we speculate that *MsDCS1* is solely responsible for production of corynanthe-type alkaloids with (20*S*)-stereochemistry in kratom (**Figure S15**).

These seven amino acids may collectively affect the orientation in which dehydrogeissoschizine (**15**) binds in the enzyme active site, which would in turn control tautomerization and protonation of **16** to either (20*S*)-**17a** or (20*R*)-**17b** (**Scheme 2b; Figure S16**). The model of the active site did not contain an amino acid that would be appropriately positioned to catalyze this stereoselective protonation, suggesting that a bound water molecule may be responsible, as previously proposed for other monoterpene indole alkaloid reductases.²¹ This mutational analysis lays the foundation for metabolic engineering strategies to improve production of mitragynine (**1**); for example, *MsDCS2* could be knocked out or mutated in kratom to generate plants with increased levels of alkaloids with (20*S*)-stereoconfiguration.

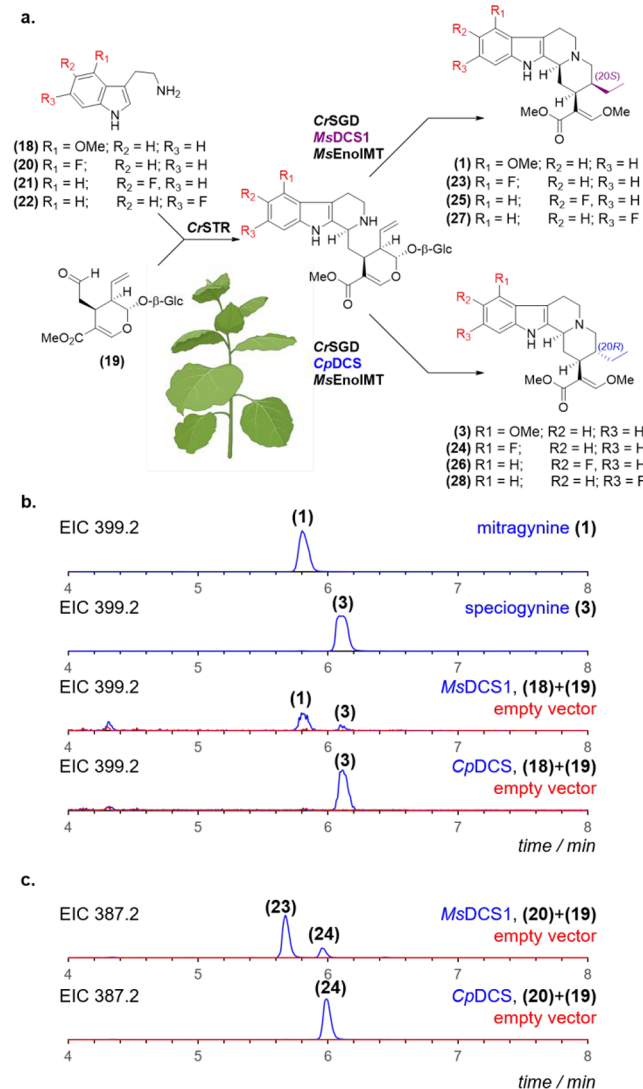
Completion of mitragynine (**1**) and speciogynine (**3**) biosynthesis requires methoxylation at C-9 of **5ab** (**Scheme 1b**).²² Since early pathway genes are expressed in roots, while **1** is found exclusively in leaves, it is difficult to predict where the genes responsible for methoxylation would be located. Therefore, we screened oxidases with a variety of expression profiles. However, although 172 candidate oxidase genes were assayed, none showed activity toward either **5a** or **5b** (**Figures S17 and S18**). Attempts to use the fungal cytochrome P450 monooxygenase *PsiH*, another oxidase known to hydroxylate this position of the indole moiety, also failed to hydroxylate **5a** or **5b** (**Figure S19**).²³

Therefore, we switched to a mutasynthetic strategy to reconstitute mitragynine (**1**) biosynthesis. *N. benthamiana* leaves were transiently expressed with *CrSTR*, *CrSGD*, *MsDCS1*, and *MsEnolMT* and infiltrated with 4-methoxytryptamine (**18**) and secologanin (**19**). Consistent with the previously observed stereoselectivity of *MsDCS1*, this afforded a mixture of **1** and **3**, with **1** as the dominant product (**Scheme 3a,b**). Exchange of *MsDCS1* with *CpDCS* solely afforded speciogynine (**3**). *In vitro* assays yielded similar results (**Figure S20**).

Notably, fluorinated mitragynine analogues have enhanced pharmacological activity.²⁴ Therefore, we assessed the potential for the biocatalytic production of fluorinated analogues of **1** and **3**. Infiltration of secologanin (**19**) and either 4F-, 5F-, or 6F-tryptamine (**20–22**), along with *CrSTR*, *CrSGD*, *MsDCS1*, and *MsEnolMT* in *N. benthamiana*, afforded compounds that corresponded to the expected fluorinated analogues (**23–28**) as evidenced by HRMS (**Scheme 3a,c; Figures S21–S26**). Although attempts to isolate these compounds in quantities sufficient for NMR analysis failed, this sets the stage for exploring more efficient yeast-based strategies for mitragynine analogue engineering.

In conclusion, we elucidated the key enzymatic steps for the production of corynanthe-type alkaloids in kratom. Mutagenesis experiments suggest a mechanism that is responsible for the control of the stereochemistry at the crucial C-20 position. These discoveries will enable targeted genome editing in kratom to fine-tune alkaloid profiles. Given the recent advent of yeast expression systems for the production of monoterpene indole alkaloids,²⁵ we anticipate that these enzymes will enable development of robust production platforms for mitragynine, speciogynine, and related analogues.

Scheme 3. (a) *N. benthamiana* Infiltration Strategy; and (b, c) EICs of Methanolic Extracts from the Transient Expression of *CrSTR*, *CrSGD*, *MsEnolMT*, and Indicated ADH Enzymes with Different Tryptamine Analogues



ASSOCIATED CONTENT

Supporting Information

The Supporting Information is available free of charge at <https://pubs.acs.org/doi/10.1021/jacs.2c13644>.

Detailed methods and materials and additional figures and data including chemical structures, LCMS results, extracted ion chromatograms, sequence alignments, pairwise sequence identities, MS/MS data, and Geneious results ([PDF](#))

AUTHOR INFORMATION

Corresponding Author

Sarah E. O'Connor – Department of Natural Product Biosynthesis, Max Planck Institute for Chemical Ecology, 07745 Jena, Germany; orcid.org/0000-0003-0356-6213; Email: oconnor@ice.mpg.de

Authors

Carsten Schotte — Department of Natural Product Biosynthesis, Max Planck Institute for Chemical Ecology, 07745 Jena, Germany

Yindi Jiang — Department of Natural Product Biosynthesis, Max Planck Institute for Chemical Ecology, 07745 Jena, Germany; Present Address: Y.J.: CAS Key Laboratory of Quantitative Engineering Biology, Shenzhen Institute of Synthetic Biology, Shenzhen Institute of Advanced Technology, Chinese Academy of Sciences, Shenzhen, China

Dagny Grzech — Department of Natural Product Biosynthesis, Max Planck Institute for Chemical Ecology, 07745 Jena, Germany;  orcid.org/0000-0001-5575-2582

Thu-Thuy T. Dang — Department of Natural Product Biosynthesis, Max Planck Institute for Chemical Ecology, 07745 Jena, Germany; Present Address: T.-T.T.D.: Department of Chemistry, Irving K. Barber Faculty of Science, University of British Columbia, Kelowna, British Columbia, Canada;  orcid.org/0000-0002-6459-3664

Larissa C. Laforest — Plant Molecular and Cell Biology Program, University of Florida, Gainesville, Florida 32606, United States

Francisco León — Department of Medicinal Chemistry, College of Pharmacy, University of Florida, Gainesville, Florida 32610, United States; Present Address: F.L.: Department of Drug Discovery and Biomedical Sciences, College of Pharmacy, University of South Carolina, Columbia, SC 29208, USA;  orcid.org/0000-0002-5064-2381

Marco Mordini — Department of Medicinal Chemistry, College of Pharmacy, University of Florida, Gainesville, Florida 32610, United States; Present Address: M.M.: Laboratory for Neglected Disease Drug Discovery, College of Science, Department of Chemistry and Chemical Biology, Northeastern University, 02115 Boston, USA;  orcid.org/0000-0001-5725-0439

Satya Swathi Nadakuduti — Plant Molecular and Cell Biology Program, University of Florida, Gainesville, Florida 32606, United States; Department of Environmental Horticulture, University of Florida, Gainesville, Florida 32606, United States;  orcid.org/0000-0002-0831-3760

Christopher R. McCurdy — Department of Medicinal Chemistry, College of Pharmacy, University of Florida, Gainesville, Florida 32610, United States;  orcid.org/0000-0001-8695-2915

Complete contact information is available at:

<https://pubs.acs.org/10.1021/jacs.2c13644>

Author Contributions

[†]C.S. and Y.J. contributed equally.

Funding

Open access funded by Max Planck Society.

Notes

The authors declare no competing financial interest.

ACKNOWLEDGMENTS

We gratefully acknowledge Delia Ayled Serna Guerrero, Sarah Heinicke, and Maritta Kunert for assistance with mass spectrometry. Jens Wurlitzer is thanked for help with molecular cloning. Eva Rothe and the MPI-CE greenhouse team is thanked for taking care of plants. Carlos E. Rodríguez

López is kindly thanked for help with bioinformatics. Maite Colinas, Prashant Sonawane, Chloe Langley, and Matilde Florea are kindly thanked for helpful discussion and advice on methodology. This work was supported by grants from the European Research Council (788301) and the Max Planck Society. A portion of this study was supported by UG3DA048353 and R01DA047855 grants from the National Institute on Drug Abuse and the University of Florida Clinical and Translational Science Institute, which is supported in part by the NIH National Center for Advancing Translational Sciences under award number UL1TR001427. The plant art in Figures 1 and 2 and Schemes 2 and 3 was created with BioRender.com. The heatmap in Scheme 2 was created with Morpheus (<https://software.broadinstitute.org/morpheus>).

ABBREVIATIONS

ADH, alcohol dehydrogenase; Cr, *Catharanthus roseus*; Cp, *Cinchona pubescens*; DCS, dihydrocorynantheine synthase; EIC, extracted ion chromatogram; FPKM, fragments per kilobase of exon per million of mapped fragments; GES, geraniol synthase; G8H, geraniol 8-hydroxylase; GOR, 8-hydroxygeraniol oxidoreductase; GPP, geranylpyrophosphate; ISY, iridoid synthase; hMOR, human μ -opioid receptor; HRMS, high-resolution mass spectrometry; Ms, *Mitragyna speciosa*; NADPH, nicotinamide adenine dinucleotide phosphate; SAM, S-adenosyl-methionine; SGD, strictosidine glucosidase; STR, strictosidine synthase; TIC, total ion chromatogram

REFERENCES

- (1) Han, C.; Schmitt, J.; Gilliland, K. M. DARK Classics in Chemical Neuroscience: Kratom. *ACS Chem. Neurosci.* **2020**, *11* (23), 3870–3880.
- (2) Assanangkornchai, S.; Muekthong, A.; Sam-angsri, N.; Pattanasattayawong, U. The Use of *Mitragyna Speciosa* ("Krathom"), an Addictive Plant, in Thailand. *Subst. Use Misuse* **2007**, *42* (14), 2145–2157.
- (3) Cinosi, E.; Martinotti, G.; Simonato, P.; Singh, D.; Demetrovics, Z.; Roman-Urestarazu, A.; Bersani, F. S.; Vicknasingam, B.; Piazzon, G.; Li, J.-H.; Yu, W.-J.; Kapitány-Fövény, M.; Farkas, J.; Di Giannantonio, M.; Corazza, O. Following "the Roots" of Kratom (*Mitragyna Speciosa*): The Evolution of an Enhancer from a Traditional Use to Increase Work and Productivity in Southeast Asia to a Recreational Psychoactive Drug in Western Countries. *BioMed. Res. Int.* **2015**, *2015*, 1–11.
- (4) Grundmann, O. Patterns of Kratom Use and Health Impact in the US—Results from an Online Survey. *Drug Alcohol Depend.* **2017**, *176*, 63–70.
- (5) Swogger, M. T.; Smith, K. E.; Garcia-Romeu, A.; Grundmann, O.; Veltri, C. A.; Henningfield, J. E.; Busch, L. Y. Understanding Kratom Use: A Guide for Healthcare Providers. *Front. Pharmacol.* **2022**, *13*, 801855.
- (6) Schimmel, J.; Amioka, E.; Rockhill, K.; Haynes, C. M.; Black, J. C.; Dart, R. C.; Iwanicki, J. L. Prevalence and Description of Kratom (*Mitragyna Speciosa*) Use in the United States: A Cross-sectional Study. *Addiction* **2021**, *116* (1), 176–181.
- (7) (a) Flores-Bocanegra, L.; Raja, H. A.; Graf, T. N.; Augustinović, M.; Wallace, E. D.; Hematian, S.; Kellogg, J. J.; Todd, D. A.; Cech, N. B.; Oberlies, N. H. The Chemistry of Kratom [*Mitragyna Speciosa*]: Updated Characterization Data and Methods to Elucidate Indole and Oxindole Alkaloids. *J. Nat. Prod.* **2020**, *83* (7), 2165–2177. (b) Nguyen, T.-A. M.; Grzech, D.; Chung, K. C.; Xia, Z.; Nguyen, T.-D.; Dang, T. T. T. Discovery of a Cytochrome P450 Enzyme Catalyzing the Formation of Spirooxindole Alkaloid Scaffold in Kratom. *Front. Plant Sci.* **2023**, *14*, 1125158.

- (8) Matsumoto, K.; Horie, S.; Ishikawa, H.; Takayama, H.; Aimi, N.; Ponglux, D.; Watanabe, K. Antinociceptive Effect of 7-Hydroxymitragynine in Mice: Discovery of an Orally Active Opioid Analgesic from the Thai Medicinal Herb *Mitragyna Speciosa*. *Life Sci.* **2004**, *74*, 2143–2155.
- (9) Takayama, H.; Ishikawa, H.; Kurihara, M.; Kitajima, M.; Aimi, N.; Ponglux, D.; Koyama, F.; Matsumoto, K.; Moriyama, T.; Yamamoto, L. T.; Watanabe, K.; Murayama, T.; Horie, S. Studies on the Synthesis and Opioid Agonistic Activities of Mitragynine-Related Indole Alkaloids: Discovery of Opioid Agonists Structurally Different from Other Opioid Ligands. *J. Med. Chem.* **2002**, *45* (9), 1949–1956.
- (10) Kruegel, A. C.; Gassaway, M. M.; Kapoor, A.; Váradí, A.; Majumdar, S.; Filizola, M.; Javitch, J. A.; Sames, D. Synthetic and Receptor Signaling Explorations of the *Mitragyna* Alkaloids: Mitragynine as an Atypical Molecular Framework for Opioid Receptor Modulators. *J. Am. Chem. Soc.* **2016**, *138* (21), 6754–6764.
- (11) Takayama, H. Chemistry and Pharmacology of Analgesic Indole Alkaloids from the Rubiaceous Plant, *Mitragyna Speciosa*. *Chem. Pharm. Bull.* **2004**, *52* (8), 916–928.
- (12) Todd, D. A.; Kellogg, J. J.; Wallace, E. D.; Khin, M.; Flores-Bocanegra, L.; Tanna, R. S.; McIntosh, S.; Raja, H. A.; Graf, T. N.; Hemby, S. E.; Paine, M. F.; Oberlies, N. H.; Cech, N. B. Chemical Composition and Biological Effects of Kratom (*Mitragyna Speciosa*): In Vitro Studies with Implications for Efficacy and Drug Interactions. *Sci. Rep.* **2020**, *10* (1), 19158.
- (13) Miettinen, K.; Dong, L.; Navrot, N.; Schneider, T.; Burlat, V.; Pollier, J.; Woittiez, L.; van der Krol, S.; Lugin, R.; Ilc, T.; Verpoorte, R.; Oksman-Caldentey, K.-M.; Martinhoia, E.; Bouwmeester, H.; Goossens, A.; Memelink, J.; Werck-Reichhart, D. The Seco-Iridoid Pathway from Catharanthus Roseus. *Nat. Commun.* **2014**, *5* (1), 3606.
- (14) Tatsis, E. C.; Carqueijeiro, I.; Dugé de Bernonville, T.; Franke, J.; Dang, T.-T. T.; Oudin, A.; Lanoue, A.; Lafontaine, F.; Stavrinides, A. K.; Clastre, M.; Courdavault, V.; O'Connor, S. E. A Three Enzyme System to Generate the Strychnos Alkaloid Scaffold from a Central Biosynthetic Intermediate. *Nat. Commun.* **2017**, *8* (1), 316.
- (15) Stavrinides, A.; Tatsis, E. C.; Foureau, E.; Caputi, L.; Kellner, F.; Courdavault, V.; O'Connor, S. E. Unlocking the Diversity of Alkaloids in Catharanthus Roseus: Nuclear Localization Suggests Metabolic Channeling in Secondary Metabolism. *Chem. Biol.* **2015**, *22* (3), 336–341.
- (16) Trenti, F.; Yamamoto, K.; Hong, B.; Paetz, C.; Nakamura, Y.; O'Connor, S. E. Early and Late Steps of Quinine Biosynthesis. *Org. Lett.* **2021**, *23* (5), 1793–1797.
- (17) Brose, J.; Lau, K. H.; Dang, T. T. T.; Hamilton, J. P.; Martins, L. do V.; Hamberger, B.; Hamberger, B.; Jiang, J.; O'Connor, S. E.; Buell, C. R. The *Mitragyna Speciosa* (Kratom) Genome: A Resource for Data-Mining Potent Pharmaceuticals That Impact Human Health. *G3 GenesGenomesGenetics* **2021**, *11* (4), jkab058.
- (18) Obeng, S.; Kamble, S. H.; Reeves, M. E.; Restrepo, L. F.; Patel, A.; Behnke, M.; Chear, N. J.-Y.; Ramanathan, S.; Sharma, A.; León, F.; Hiranita, T.; Avery, B. A.; McMahon, L. R.; McCurdy, C. R. Investigation of the Adrenergic and Opioid Binding Affinities, Metabolic Stability, Plasma Protein Binding Properties, and Functional Effects of Selected Indole-Based Kratom Alkaloids. *J. Med. Chem.* **2020**, *63* (1), 433–439.
- (19) Baek, M.; DiMaio, F.; Anishchenko, I.; Dauparas, J.; Ovchinnikov, S.; Lee, G. R.; Wang, J.; Cong, Q.; Kinch, L. N.; Schaeffer, R. D.; Millán, C.; Park, H.; Adams, C.; Glassman, C. R.; DeGiovanni, A.; Pereira, J. H.; Rodrigues, A. V.; van Dijk, A. A.; Ebrecht, A. C.; Opperman, D. J.; Sagmeister, T.; Buhlheller, C.; Pavkov-Keller, T.; Rathinaswamy, M. K.; Dalwadi, U.; Yip, C. K.; Burke, J. E.; Garcia, K. C.; Grishin, N. V.; Adams, P. D.; Read, R. J.; Baker, D. Accurate Prediction of Protein Structures and Interactions Using a Three-Track Neural Network. *Science* **2021**, *373* (6557), 871–876.
- (20) Kochnev, Y.; Hellemann, E.; Cassidy, K. C.; Durrant, J. D. Webina: An Open-Source Library and Web App That Runs AutoDock Vina Entirely in the Web Browser. *Bioinformatics* **2020**, *36* (16), 4513–4515.
- (21) Stavrinides, A.; Tatsis, E. C.; Caputi, L.; Foureau, E.; Stevenson, C. E. M.; Lawson, D. M.; Courdavault, V.; O'Connor, S. E. Structural Investigation of Heteroyohimbine Alkaloid Synthesis Reveals Active Site Elements That Control Stereoselectivity. *Nat. Commun.* **2016**, *7* (1), 12116.
- (22) Franke, J.; Kim, J.; Hamilton, J. P.; Zhao, D.; Pham, G. M.; Wiegert-Rininger, K.; Crisovan, E.; Newton, L.; Vaillancourt, B.; Tatsis, E.; Buell, C. R.; O'Connor, S. E. Gene Discovery in *Gelsemium* Highlights Conserved Gene Clusters in Monoterpene Indole Alkaloid Biosynthesis. *ChemBioChem* **2019**, *20* (1), 83–87.
- (23) Fricke, J.; Blei, F.; Hoffmeister, D. Enzymatic Synthesis of Psilocybin. *Angew. Chem., Int. Ed.* **2017**, *56* (40), 12352–12355.
- (24) Takayama, H.; Misawa, K.; Okada, N.; Ishikawa, H.; Kitajima, M.; Hatori, Y.; Murayama, T.; Wongseripipatana, S.; Tashima, K.; Matsumoto, K.; Horie, S. New Procedure to Mask the 2,3-π Bond of the Indole Nucleus and Its Application to the Preparation of Potent Opioid Receptor Agonists with a Corynanthe Skeleton. *Org. Lett.* **2006**, *8* (25), 5705–5708.
- (25) Zhang, J.; Hansen, L. G.; Gudich, O.; Viehrig, K.; Lassen, L. M. M.; Schröbbers, L.; Adhikari, K. B.; Rubaszka, P.; Carrasquer-Alvarez, E.; Chen, L.; D'Ambrosio, V.; Lehka, B.; Haidar, A. K.; Nallapareddy, S.; Giannakou, K.; Laloux, M.; Arsovská, D.; Jørgensen, M. A. K.; Chan, L. J. G.; Kristensen, M.; Christensen, H. B.; Sudarsan, S.; Stander, E. A.; Baidoo, E.; Petzold, C. J.; Wulff, T.; O'Connor, S. E.; Courdavault, V.; Jensen, M. K.; Keasling, J. D. A Microbial Supply Chain for Production of the Anti-Cancer Drug Vinblastine. *Nature* **2022**, *609* (7926), 341–347.

■ NOTE ADDED AFTER ASAP PUBLICATION

This paper was published on February 22, 2023. Scheme 2 and Figure 2 have been updated. The revised version of the paper was re-posted on March 8, 2023.

□ Recommended by ACS

Post-Cyclization Skeletal Rearrangements in Plant Triterpenoid Biosynthesis by a Pair of Branchpoint Isomerases

Ling Chuang, Jakob Franke, et al.

FEBRUARY 23, 2023

JOURNAL OF THE AMERICAN CHEMICAL SOCIETY

READ ▾

Stictamycin, an Aromatic Polyketide Antibiotic Isolated from a New Zealand Lichen-Sourced *Streptomyces* Species

Peng Hou, Jeremy G. Owen, et al.

FEBRUARY 16, 2023

JOURNAL OF NATURAL PRODUCTS

READ ▾

Reactive Azlactone Intermediate Drives Fungal Secondary Metabolite Cross-Pathway Generation

Shinji Kishimoto, Kenji Watanabe, et al.

JANUARY 27, 2023

JOURNAL OF THE AMERICAN CHEMICAL SOCIETY

READ ▾

Enzymatic *cis*-Decalin Formation in Natural Product Biosynthesis

Masao Ohashi, Yi Tang, et al.

FEBRUARY 01, 2023

JOURNAL OF THE AMERICAN CHEMICAL SOCIETY

READ ▾

Get More Suggestions >